Neutral and Cationic Palladium(II) Complexes of a Diazapyridinophane. Structure, Fluxionality, and Reactivity toward Ethylene

Simoni Plentz Meneghetti,[†,‡] Pierre J. Lutz,[‡] and Jacky Kress*[,†]

Laboratoire de Chimie des Métaux de Transition et de Catalyse, UMR du CNRS 7513, Institut Le Bel, 4 Rue Blaise Pascal, Université Louis Pasteur, 67000 Strasbourg, France, and Institut Charles Sadron, UPR du CNRS 22, 6 Rue Boussingault, 67000 Strasbourg, France

Received June 5, 2001

The palladium complexes (*t*-Bu-N_4)$PdCl_2$ (**1**), (*t*-Bu-N_4)PdMeCl (**2**), (*t*-Bu-N_4)PdMe(NCMe)$^+$-BAr_4^- (**3**), and (*t*-Bu-N_4)PdMe$(C_2H_4)^+BAr_4^-$ (**4**) [*t*-Bu-N_4 = *N*,*N*′-ditertiobutyl-2,11-diaza[3.3]-(2,6)pyridinophane, Ar = 3,5-$(CF_3)_2$-C_6H_3] have been synthesized and characterized by VT ^{1}H NMR and X-ray (for **1** and **3**) analysis. The macrocyclic ligand is only bi- or tridentate, both coordination modes coexisting in solution for **1** and **3**. Cationic methyl-ethylene complex **4** decomposes readily through insertion of ethylene into the Pd−Me bond, and ethylene polymerization with use of **1** (in the presence of MAO) or **3** as catalysts is therefore precluded. Complexes **1**, **3**, and **4** are fluxional, the *t*-Bu-N_4 ligand undergoing an $\eta^2-\eta^3$ oscillatory process ($\Delta G^{\ddagger}$ = 14.1−14.9 kcal mol^{-1}) as well as hindered rotation of the *t*-Bu substituent of the coordinated amine function around the corresponding N−C bond ($\Delta G^{\ddagger}$ = 8.8−10.1 kcal mol^{-1}).

Introduction

Complexation studies of *N*,*N*′-dialkyl-2,11-diaza[3.3]-(2,6)pyridinophanes (R−N_4) have led to a number of octahedral transition metal complexes in which the tetraazamacrocyclic ligands are most often tetradentate.[1] Other coordination modes have been reported in only two instances.[2] Since palladium(II) is less prone to axial interactions, it seemed likely that complexation to this metal will generate different coordination modes and geometries and that bidentate coordination via the two pyridyl functions may, in particular, be expected. Furthermore, cationic alkyl derivatives of this type could be considered as analogues of the square-planar diimine complexes that behave as efficient molecular catalysts for the polymerization of olefins.[3] The key characteristic of these catalysts is steric protection of the axial coordination sites by the ancillary diimine ligands, and we wished to probe if cyclic ligands such as the diazapyridinophanes were able to ensure a similar protection and to give rise to comparable insertion chemistry. The known *t*-Bu-N_4 derivative,[1c] which contains bulky *tert*-butyl substituents on the two amino nitrogen atoms, was chosen to favor such steric effects and weaken yet possible palladium−amine interactions. We describe here the outcome of these investigations.

Scheme 1

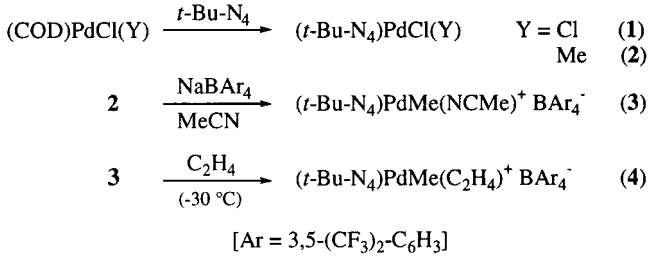

Results and Discussion

Complexes **1**, **2**, and **3** were synthesized following procedures previously described for the palladium−diimine analogues[3] (Scheme 1; 80, 65, and 67% yield, respectively). Orange crystals of **1** and **3** were obtained respectively from a $CHCl_3$ or a MeCN solution and analyzed by X-ray crystallography (Figures 1 and 2). In the solid state, **1** consists of square-planar molecules of

* E-mail: jkress@chimie.u-strasbg.fr.
† Laboratoire de Chimie des Métaux de Transition et de Catalyse.
‡ Institut Charles Sadron.

(1) (a) Fronczek, F. R.; Mamo, A.; Pappalardo, S. *Inorg. Chem.* **1989**, *28*, 1419. (b) Sakaba, H.; Kabuto, C.; Horino, H.; Arai, M. *Bull. Chem. Soc. Jpn.* **1990**, *63*, 1822. (c) Che, C.-M.; Li, Z.-Y.; Wong, K.-Y.; Poon, C.-K.; Mak, T. C. W.; Peng, S.-M. *Polyhedron* **1994**, *13*, 771. (d) Krüger, H.-J. *Chem. Ber.* **1995**, *128*, 531. (e) Koch, W. O.; Krüger, H.-J. *Angew. Chem., Int. Ed. Engl.* **1995**, *34*, 2671. (f) Kelm, H.; Krüger, H.-J. *Inorg. Chem.* **1996**, *35*, 3533. (g) Koch, W. O.; Schünemann, V.; Gerdan, M.; Trautwein, A. X.; Krüger, H.-J. *Chem. Eur. J.* **1998**, *4*, 686 and 1255. (h) Plentz Meneghetti, S.; Lutz, P. J.; Fischer, J.; Kress, J. *Polyhedron* **2001**, *20*, 2705.

(2) (a) Kelm, H.; Krüger, H.-J. *Eur. J. Inorg. Chem.* **1998**, 1381. (b) Koch, W. O.; Kaiser, J. T.; Krüger, H.-J. *Chem. Commun.* **1997**, 2237.

(3) (a) Johnson, L. K.; Killian, C. M.; Brookhart, M. *J. Am. Chem. Soc.* **1995**, *117*, 6414. (b) Johnson, L. K.; Mecking, S.; Brookhart, M. *J. Am. Chem. Soc.* **1996**, *118*, 267. (c) Deng, L.; Woo, T. K.; Cavello, L.; Margl, P. M.; Ziegler, T. *J. Am. Chem. Soc.* **1997**, *119*, 6177. (d) Schleis, T.; Heinemann, J.; Spaniol, T. P.; Mulhaupt, R.; Okuda, J. *Inorg. Chem. Commun.* **1998**, *1*, 431. (e) Musaev, D. G.; Froese, R. D. J.; Morokuma, K. *Organometallics* **1998**, *17*, 1850. (f) Mecking, S.; Johnson, L. K.; Wang, L.; Brookhart, M. *J. Am. Chem. Soc.* **1998**, *120*, 888. (g) Guan, Z.; Cotts, P. M.; McCord, E. F.; McLain, S. J. *Science* **1999**, *283*, 2059. (h) Ittel, S. D.; Johnson, L. K.; Brookhart, M. *Chem. Rev.* **2000**, *100*, 1169. (i) Tempel, D. J.; Johnson, L. K.; Huff, R. L.; White, P. S.; Brookhart, M. *J. Am. Chem. Soc.* **2000**, *122*, 6686. (j) Gottfried, A. C.; Brookhart, M. *Macromolecules* **2001**, *34*, 1140. (k) Plentz Meneghetti, S.; Kress, J.; Lutz, P. J. *Macromol. Chem. Phys.* **2000**, *201*, 1823. (l) Held, A.; Mecking, S. *Chem. Eur. J.* **2000**, *6*, 4623. (m) Mecking, S. *Coord. Chem. Rev.* **2000**, *203*, 325.

10.1021/om010475e CCC: $20.00
Publication on Web 10/20/2001

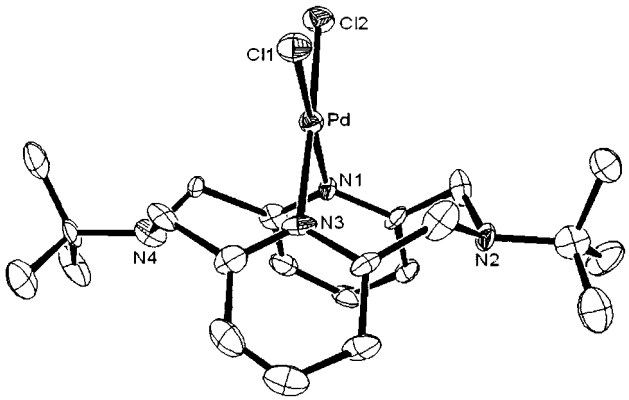

Figure 1. ORTEP drawing of **1**. Thermal ellipsoids are drawn at the 50% probability level. Hydrogen atoms and solvent molecules are omitted for clarity. Selected bond distances (Å) and angles (deg): Pd−N(1) = 2.041(8), Pd−N(3) = 2.054(7), Pd−Cl(1) = 2.314(3), Pd−Cl(2) = 2.307(3), N(1)−Pd−N(3) = 80.73(9), Cl(1)−Pd−Cl(2) = 93.41(3).

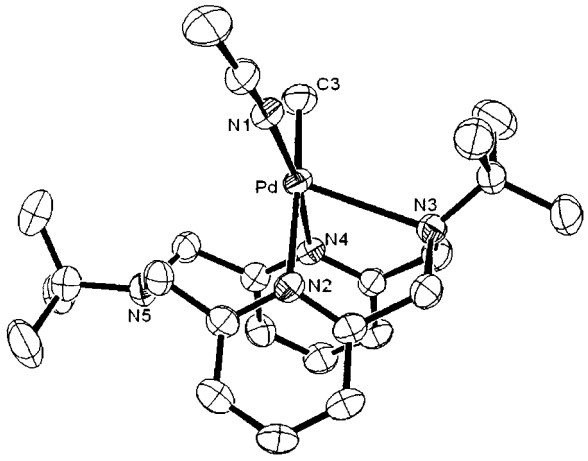

Figure 2. ORTEP drawing of **3**. Thermal ellipsoids are drawn at the 50% probability level. Hydrogen atoms and the BAr_4^- counteranion are omitted for clarity. Selected bond distances (Å) and angles (deg): Pd−N(1) = 2.022(4), Pd−N(2) = 2.200(4), Pd−N(3) = 2.670(4), Pd−N(4) = 2.065(3), Pd−C(3) = 2.017(5), N(2)−Pd−N(4) = 77.1(1), C(3)−Pd−N(1) = 88.5(2), N(2)−Pd−N(3) = 73.3(2), N(4)−Pd−N(3) = 75.6(2).

pseudo-C_{2v} symmetry, in which the *t*-Bu-N_4 ligand adopts the desired bidentate coordination mode and retains the *syn* chair−chair conformation of the free macrocycle.[1c] Short Pd−N_{py} bond distances (N_{py} = pyridyl nitrogen atom) indicate the strength of the interaction between palladium and the two pyridine functions. As for the tetradentate diazapyridinophane ligands with conformation *syn* boat−boat,[1] the N_{py}−M−N_{py} angle is small (80.7°) and the dihedral angle that the two pyridine rings form with each other even smaller (ca. 56°), although still much larger than in the free ligand.[1c] The two *tert*-butyl groups are aligned along the N(2)−N(4) axis, providing thereby only limited steric protection to the two axial sites of the complex.[4]

The molecular structure of cationic **3** in the solid state (Figure 2) is different insofar as the more electron-deficient palladium center interacts furthermore apically with one of the two amine functions of *t*-Bu-N_4, becoming thereby five-coordinate and surrounded by a distorted square-pyramidal coordination geometry. The tridentate macrocyclic ligand adopts the *syn* chair−boat conformation. However, the palladium−amine interaction is weak [Pd−N(3) = 2.67 Å], so that the macrocycle is much less twisted than in hexacoordinate (η^4-*t*-Bu-N_4)$NiBr_2$ for instance,[1h] and the *t*-Bu substituent of the coordinated amine is directed between the two equatorial ligands (Me and NCMe in this case). It yet slightly displaces the Pd atom from the basal plane, toward N(3), and pushes the NCMe framework out of this plane, in the opposite direction. The Pd−N_{py} bonds are weaker than in **1**, especially the one *trans* to the Me ligand, and the angle between the two pyridine rings is reduced to ca. 48°. In contrast, the Pd−N(1) distance between palladium and acetonitrile is remarkably short.

Scheme 2

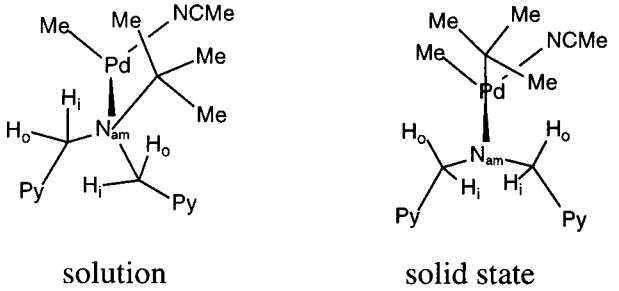

solution solid state

In solution (CD_2Cl_2), the two types of structures described above, which will be designated by **a** (four-coordinate, η^2-ligand) and **b** (five-coordinate, η^3-ligand), coexist for **1** and **3** in the temperature-independent ratio of ca. 2:3 and 3:4, respectively, whereas **2** exists as a single isomer of type **a**. This can be clearly deduced from the low-temperature ^{1}H NMR spectra of the three compounds, in which the half-macrocycles containing a coordinated amine function are easily distinguished from those containing a free amine function,[5] while both fragments constitute useful symmetry probes. For **3a**,**b**, full assignment of the spectra is based on a NOESY experiment that enabled moreover to show that coordination of the amine function in **3b** leads to a significant twist of the corresponding ligand half, through which the *t*-Bu_c[7] group is directed toward the NCMe ligand and not between the Me and NCMe ligands as in the solid state (Scheme 2). *t*-Bu_c is indeed found near to $CH_{c,Me,i}H$ on one hand and $CH_{c,NCMe,o}H$ on the other hand. This shows that the Pd−N_{am} interaction in **3b** (N_{am} = amino nitrogen atom) is stronger in solution than in the solid state and becomes closer to that observed in (η^4-*t*-Bu-N_4)$NiBr_2$.[1h]

Complex **3** reacts smoothly with 5 equiv of ethylene in CD_2Cl_2 at −30 °C to yield complex **4** (Scheme 1), as

(4) The molecular structure of (Ts-N_4)$PdCl_2$ (Ts = $SO_2C_6H_4$-4-Me, orange crystals) is similar. Pd−N_{py} = 2.14(1) Å, Pd−Cl = 2.251(6) Å.

(5) The chemical shift of the inner CH_iH_o protons is particularly characteristic. If the adjacent nitrogen atom is bound to palladium, these protons are shielded by the pyridine rings that are then in close proximity (δ 3.62 for **1b**, 3.64/3.30 for **3b**). If the nitrogen atom is not bound, they become near an apical site of palladium and the paramagnetic anisotropy of this atom[6] is shifting their resonances downfield (δ 6.11 for **1a**, 6.68 for **1b**, 5.64/5.54 for **2a**, 5.03/5.00 for **3a**, 5.71/5.36 for **3b**). This latter effect is also observed for the *t*-Bu substituent of the coordinated amine functions [δ 1.64 (−26 °C) and 1.40 (−60 °C) for **1b** and **3b**, respectively].

(6) Miller, R. G.; Stauffer, R. D.; Fahey, D. R.; Parnell, D. R. *J. Am. Chem. Soc.* **1970**, *92*, 1511.

(7) Indexes *i* or *o*, *f* or *c*, and *Cl*, *Me*, or *NCMe* designate protons located respectively *i*nside or *o*utside the macrocyclic ring, beside the *f*ree or the *c*oordinated amine function, and on the side of the *Cl*, *Me*, or *NCMe* ligands.

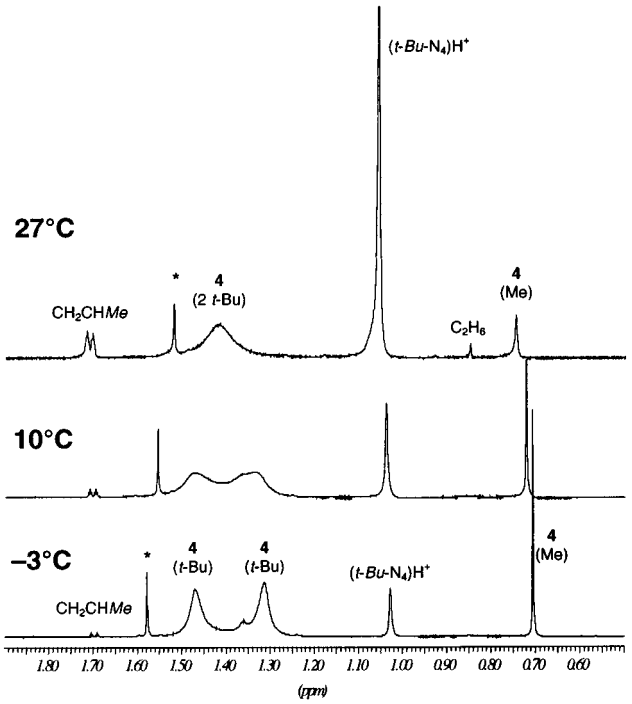

Figure 3. Modification of the ^{1}H NMR spectrum (500 MHz, 1.9−0.5 ppm) of **4** (+ C_2H_4) in CD_2Cl_2 on raising progressively the temperature from −3 to 27 °C (* = H_2O).

shown by in situ ^{1}H NMR analysis. Isomers **3a** and **3b** are converted simultaneously and almost quantitatively within 1 h, releasing 1 equiv of acetonitrile. The spectrum of the single isomer detected for the cationic ethylene complex **4** is characteristic of the square-pyramidal geometry of type **b**. The apical Pd−N_{am} interaction is probably favored, with respect to **3**, by the stronger electron-withdrawing nature of the C_2H_4 ligand. Its strength in **4** is further confirmed by an ^{1}H−^{1}H COSY experiment that reveals significant distortion of the macrocycle around the coordinated amine function[8] and allows more precise assignment. Overall, it follows the order **4** > **3** > **1** > **2**, in agreement with decreasing electron deficiency at palladium in this series. The C_2H_4 ligand gives rise at −30 °C to an AA′BB′ multiplet centered at δ 4.29 and is probably rotating quickly around the palladium−olefin bond axis.

On raising the temperature above 0 °C, **4** decomposes readily to yield ca. 1 equiv of propene and of the protonated ligand salt (*t*-Bu-N_4)H$^+$$BAr_4^-$,[1h] together with traces of ethane (Figure 3). Obviously, insertion of ethylene into the palladium−methyl bond is fast at these temperatures, but subsequent β-hydride elimination in the resultant palladium-*n*-propyl complex is even faster, and chain growth via further insertion steps is hence precluded. Concomitant formation of (*t*-Bu-N_4)H$^+$ BAr_4^- suggests that the migrating hydrogen is trapped by the macrocyclic ligand, via a mechanism that has not been investigated further. Since a deposit of metallic palladium is formed simultaneously, and decomposition of **3** at room temperature in CD_2Cl_2, which leads similarly (although much more slowly) to the protonated salt in high yield, is accelerated by ambient light, a radical mechanism is probably involved.

Figure 3 shows also that the two *t*-Bu singlets of **4** broaden above −10 °C and coalesce at ca. 18 °C into a single resonance at δ 1.43 at 27 °C. In the lower field region, all other *t*-Bu-N_4 signals, except the two triplets due to the para-pyridyl protons, broaden similarly before they coalesce two by two. Furthermore, the two components of the AA′BB′ system observed for the ethylene ligand coalesce into a singlet at 8 °C.[9] The half-macrocycle containing the coordinated amine function is hence equilibrating with the other half, which indicates the occurrence in **4** of a dynamic oscillatory process through which the apically bound nitrogen atom is reversibly dissociated from the palladium center, and the conformation of the macrocyclic ligand changes from *syn* chair−boat to *syn* chair−chair. The free activation energy of this η^2−η^3 exchange process was calculated with use of the Eyring equation:[10] $\Delta G^{\ddagger} = 14.1 \pm 0.2$ kcal mol^{-1}. A similar fluxional behavior is found for compounds **1** and **3**, for which it leads moreover to equilibration of the two isomers **a** and **b**,[11] with an activation energy of 14.9 ± 0.2 and 14.5 ± 0.2 kcal mol^{-1} for **1b** (in C_6D_5Br) and **3b** (in CD_2Cl_2), respectively.[10,12] Surprisingly, the $\Delta G^{\ddagger}$ values seem to decrease slightly with strengthening of the Pd−N_{am} bond.

On lowering the temperature of pentacoordinate **1b**, **3b**, and **4** to −90 °C in CD_2Cl_2, the ^{1}H NMR singlet assigned to *t*-Bu_c[7] splits into two components at δ 1.72 (6H)/1.30 (3H), 1.59 (3H)/1.28 (6H), and 1.62 (3H)/1.23 (6H), respectively. The other resonances are not significantly modified, except the multiplet due to the ethylene ligand of **4**, which is markedly broadened but not yet split into a more complex pattern. As the temperature is raised, each pair of singlets broadens and then collapses at −65, −82, and −53 °C, respectively. This is illustrated for **4** in Figure 4. Hence, rotation of *t*-Bu_c around the corresponding N_{am}−C bond is hindered in these compounds, probably as a result of steric interactions with the ligands in the basal plane (Cl, Me, NCMe, or C_2H_4). The higher rotational barrier in **4** (10.1 ± 0.2 kcal mol^{-1}),[10] in comparison with **3b** (8.8 ± 0.2 kcal mol^{-1}),[10] is consistent with the probably shorter Pd−N_{am} bond and the stronger steric constraints certainly exerted by the ethylene ligand. Broadening of the ethylene resonance at −90 °C (especially the high-field component of the multiplet) probably corresponds to slower ethylene rotation at this temperature and suggests that *t*-Bu_c rotation may be concerted with hindered ethylene rotation about the Pd−ethylene bond axis, in a gear-wheels-type process.

Further, the fact that only one methyl group of *t*-Bu_c is unshielded in the limiting spectrum of **3b** and **4** (Figure 4) is in agreement with the twisted conformation

(8) The two $H_{m\text{-}Py}$ protons of one of the pyridine rings (δ 6.86 and 7.13) are coupled with both $H_{c,i}$ and $H_{c,o}$ protons of the neighboring CH_2 group (δ 3.51 and 4.59, respectively), whereas those of the other pyridine ring (δ 6.97 and 7.02) are coupled with the corresponding $H_{c,o}$ proton (δ 4.76), but not with the $H_{c,i}$ one (δ 3.68).

(9) They do not collapse, however, with the singlet due to free ethylene (δ 5.39), showing that chemical exchange between bound and unbound ethylene is slow on the NMR time scale and that the palladium−ethylene interaction is rather strong.

(10) Günther, H. *La spectroscopie de RMN*; Masson: Paris, France, 1993.

(11) For **3a** and **3b** for instance, not only the η^2- and η^3-*t*-Bu-N_4 resonances coalesce, but also the two Me (at 25 °C) and the two NCMe ones (at 13 °C). No exchange between bound and unbound acetonitrile is yet detected at these temperatures, in agreement with the strength of the corresponding palladium−nitrogen bond in the solid state. See also ref 2a.

(12) Shanan-Atidi, H.; Bar-Eli, K. H. *J. Phys. Chem.* **1970**, *74*, 961.

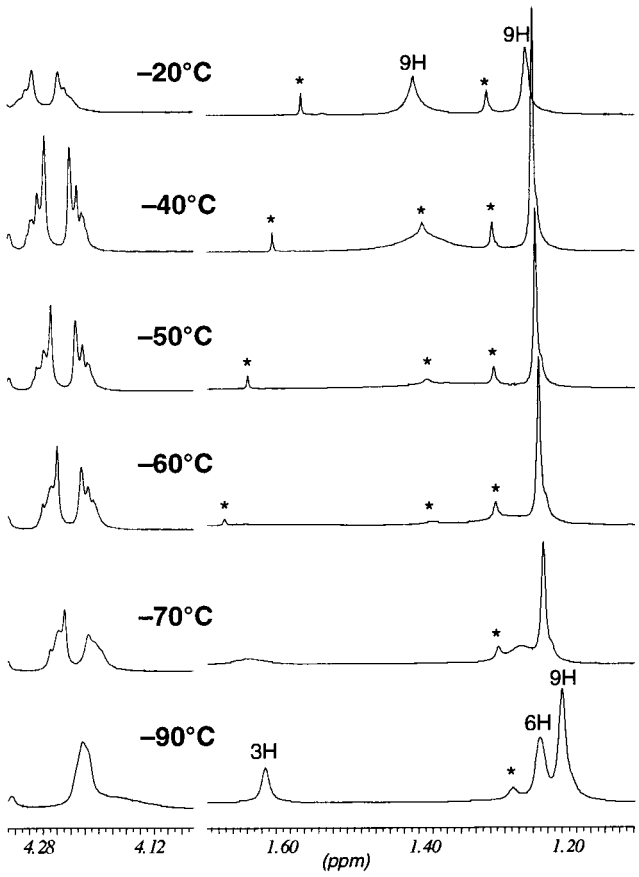

Figure 4. Variable-temperature ^{1}H NMR spectra (500 MHz) of **4** in CD_2Cl_2. Only the ethylene and the *t*-Bu regions are shown. The sample is contaminated with low amounts of **3a**,**b** (**3b** is also fluxional in this temperature range) and water (*).

of the macrocyclic ligand in these compounds in solution [the unshielding is assigned to paramagnetic anisotropy of palladium,[6] and it was shown in the case of (η^4-*t*-Bu-N_4)$NiBr_2$ that a single Me group of *t*-Bu_c is located in proximity to palladium when *t*-Bu-N_4 is twisted].[1h] For **1b**, on the contrary, there are two equally unshielded Me groups. This suggests that the η^3-macrocycle is less twisted in this compound, the Pd−N_{am} bond being weaker, and that in the ground state *t*-Bu_c is probably positioned approximately as in **3b** in the solid state (Figure 2, Scheme 2). The higher barrier to rotation in **1b** ($\Delta G^{\ddagger} = 9.5 \pm 0.2$ kcal mol^{-1}),[10] with respect to **3b**, may also be explained in this way.

Ethylene polymerization or oligomerization attempts with use of **1** (in the presence of MAO, rt, 6 bar, 2 h) or **3** (rt, 6 bar, 18 h) as catalysts were unsuccessful. In both cases, pressurization with ethylene was followed by quasi-immediate precipitation of metallic palladium. Also hex-1-ene induces fast decomposition of **3** at room temperature. This is slowed at −10 °C, but again no polymer or oligomer could be detected at this temperature. These results are fully consistent with the instability of the cationic ethylene complex **4**.

Conclusions

This work describes the first palladium complexes of a diazapyridinophane, as well as the first organometallic compounds involving such macrocyclic ligands. A new bidentate coordination mode is observed in some of the complexes, while the macrocycle is tridentate in others, and both four- and five-coordinate structures can coexist in solution, where they interchange slowly on the NMR time scale. In the latter, the presence of a bulky *t*-Bu group on the bound amino nitrogen atom leads to more or less distortion of the ligand frame and to hindered rotation of this *t*-Bu group around the N_{am}−C bond. The cationic methyl complex **3** binds ethylene and inserts it into its Pd−C bond, but subsequent decomposition with formation of (*t*-Bu-N_4)$H^+BAr_4^-$ precludes its use as a polymerization catalyst. Further studies in this field should therefore be directed toward ligands that are less prone to protonation.

Experimental Section

General Procedures. Although the compounds described herein are not significantly air-sensitive, most experiments were performed on a vacuum line or under an argon atmosphere using standard Schlenk techniques. Diethyl ether and hexane were dried over Na/benzophenone ketyl; dichloromethane was dried over P_2O_5, and acetonitrile over calcium hydride. The solvents were then distilled under argon. Ethylene was used as received. Hex-1-ene was refluxed over sodium and distilled trap-to-trap under vacuum. *t*-Bu-N_4,[1c] (COD)$PdCl_2$,[13] (COD)PdMeCl,[14] and $NaBAr_4$[15] were prepared according to the procedures outlined in the literature. Methylaluminoxane (MAO) was purchased as a 10% toluene solution from Aldrich. ^{1}H and ^{13}C NMR spectra were recorded on a Bruker ARX-500 spectrometer. Chemical shifts are reported in ppm versus $SiMe_4$ and were determined by reference to the residual solvent peaks. Elemental analyses were performed by the Service de Caractérisation de l'Institut Charles Sadron (Strasbourg).

Compound (*t*-Bu-N_4)$PdCl_2$ (1). A 1.00 g sample of (COD)$PdCl_2$ (3.50 mmol) and 1.23 g of *t*-Bu-N_4 (3.50 mmol) were dissolved in CH_2Cl_2 at room temperature, and the solution was stirred for 24 h. The solvent was then evaporated under vacuum to yield an orange powder that was recrystallized from $CHCl_3$ or CH_2Cl_2. Orange crystals of **1** were obtained in 80% yield. ^{1}H NMR (CD_2Cl_2, −26 °C):[7] **1a** δ 7.63 (t, 2H, H_{p-Py}), 7.17 (d, 4H, H_{m-Py}), 6.11 (d, 4H, CH_iH_o), 4.79 (d, 4H, CH_iH_o), 1.34 (s, 18H, *t*-Bu); **1b** δ 7.56 (t, 2H, H_{p-Py}), 7.13 (d, 2H, $H_{m-Py,f}$), 7.02 (d, 2H, $H_{m-Py,c}$), 6.68 (d, 2H, $CH_{f,i}CH_{f,o}$), 4.85 (d, 2H, $CH_{f,i}CH_{f,o}$), 4.81 (d, 2H, $CH_{c,i}CH_{c,o}$), 3.62 (d, 2H, $CH_{c,i}CH_{c,o}$), 1.64 (s, 9H, *t*-Bu_c), 1.26 (s, 9H, *t*-Bu_f). Anal. Calcd for $C_{22.4}H_{32.4}Cl_{3.2}N_4Pd$: C, 46.58; H, 5.65; N, 9.70. Found: C, 46.29; H, 5.65; N, 9.32.

Compound (*t*-Bu-N_4)PdMeCl (2). A 1.00 g sample of (COD)PdMeCl (3.8 mmol) and 1.33 g of *t*-Bu-N_4 (3.8 mmol) were dissolved in 25 mL of diethyl ether at room temperature, and the solution was stirred for 24 h. The solvent was then evaporated under vacuum to yield a yellow powder that was recrystallized by addition of hexane to a CH_2Cl_2 solution. Complex **2** was obtained as a yellow solid in 65% yield. It is rather unstable at room temperature, being slowly converted, in dichloromethane as well as in bromobenzene, into **1** and an unidentified unstable compound that is probably (*t*-Bu-N_4)$PdMe_2$. Decomposition of the latter yields metallic palladium and the protonated macrocycle, as for **3** and **4**. ^{1}H NMR (CD_2Cl_2, −20 °C):[7] δ 7.46 and 7.40 (t, 1H, $H_{p-Py,Cl}$ and $H_{p-Py,Me}$), 7.06 and 7.00 (d, 2H, $H_{m-Py,Cl}$ and $H_{m-Py,Me}$), 5.64 and 5.54, (d, 2H, CH_2, $H_{Cl,i}$ and $H_{Me,i}$), 4.63 and 4.49 (d, 2H, CH_2, $H_{Cl,o}$ and $H_{Me,o}$), 1.34 (s, 18H, *t*-Bu), 0.60 (s, 3H, Pd-Me). Anal. Calcd for $C_{23}H_{35}ClN_4Pd$: C, 54.20; H, 6.90; N, 11.00. Found: C, 53.86; H, 6.90; N, 10.64.

(13) Drew, D.; Doyle, J. R. *Inorg. Synth.* **1972**, *13*, 47.
(14) Rulke, R. E.; Ernsting, J. M.; Spek, A. L.; Elsevier, C. J.; van Leeuwen, P. W. N. M.; Vrieze, K. *Inorg. Chem.* **1993**, *32*, 5769.
(15) Bahr, S. R.; Boudjouk, P. *J. Org. Chem.* **1992**, *57*, 5545.

Table 1. X-ray Experimental Data for 1 and 3

	1·2$CHCl_3$	**3**
formula	$C_{24}H_{34}Cl_8N_4Pd$ $C_{22}H_{32}Cl_2N_4Pd$·2$CHCl_3$	$C_{57}H_{50}BF_{24}N_5Pd$ $C_{25}H_{38}N_5Pd$·$C_{32}H_{12}BF_{24}$
molecular wt	768.59	1378.24
cryst syst	monoclinic	triclinic
space group	*Cc*	$P\bar{1}$
a (Å)	19.7343(6)	12.0376(4)
b (Å)	11.0721(4)	12.5869(4)
c (Å)	14.6680(3)	20.0815(7)
α (deg)		88.554(5)
β (deg)	91.977(5)	88.446(5)
γ (deg)		81.812(5)
V (Å^3)	3203.1(3)	3009.8(3)
Z	4	2
color	orange	yellow
crystal dimens (mm)	0.20 × 0.14 × 0.08	0.20 × 0.16 × 0.14
D_{calc} (g cm^{-3})	1.59	1.52
*F*000	1552	1388
μ (mm^{-1})	1.269	0.424
temperature (K)	173	173
wavelength (Å)	0.71073	0.71073
radiation	Mo Kα graphite monochromated	Mo Kα graphite monochromated
diffractometer	KappaCCD	KappaCCD
scan mode	phi scans	phi scans
hkl limits	0,25/0,14/−19,19	0,15/−15,16/−25,26
θ limits (deg)	2.5/27.48	2.5/27.50
no. of data measd	3844	13 381
no. of data with $I > 3\sigma(I)$	3165	8033
weighting scheme	$4F_o^2/(\sigma^2(F_o^2) + 0.0016\ F_o^4)$	$4F_o^2/(\sigma^2(F_o^2) + 0.0064\ F_o^4)$
no. of variables	332	793
R	0.027	0.054
R_w	0.036	0.079
GOF	1.212	1.425
largest peak in final difference (e Å^{-3})	1.830	1.148

Compound (*t*-Bu-N_4)PdMe(NCMe)$^+$$BAr_4^-$ (3). A 1.50 g sample of (*t*-Bu-N_4)PdMeCl (**2**) (2.9 mmol) and 2.61 g of $NaBAr_4$ (2.9 mmol) were dissolved in MeCN at room temperature, and the solution was stirred for 24 h. The solvent was then evaporated under vacuum to yield an orange powder that was recrystallized at low temperature from acetonitrile. Orange crystals of **3** were obtained in 67% yield. ^{1}H NMR (CD_2Cl_2, −60 °C):[7,16] **3a** *δ* 7.50 (t, 1H, $H_{p\text{-}Py,Me}$), 7.45 (t, 1H, $H_{p\text{-}Py,NCMe}$), 7.08 (d, 2H, $H_{m\text{-}Py,Me}$), 7.02 (d, 2H, $H_{m\text{-}Py,NCMe}$), 5.03 (d, 2H, CH_2, $H_{NCMe,i}$), 5.00 (d, 2H, CH_2, $H_{Me,i}$), 4.68 (d, 2H, CH_2, $H_{Me,o}$), 4.54 (d, 2H, CH_2, $H_{NCMe,o}$), 2.26 (s, 3H, *Me*CN), 1.31 (s, 18H, *t*-Bu), 0.75 (s, 3H, Pd-Me); **3b** *δ* 7.50 (t, 1H, $H_{p\text{-}Py,Me}$), 7.42 (t, 1H, $H_{p\text{-}Py,NCMe}$), 7.12 (d, 1H, $H_{m\text{-}Py,Me,f}$), 7.03 (d, 1H, $H_{m\text{-}Py,Me,c}$), 6.98 (d, 1H, $H_{m\text{-}Py,NCMe,f}$), 6.83 (d, 1H, $H_{m\text{-}Py,NCMe,c}$), 5.71 (d, 1H, CH_2, $H_{f,NCMe,i}$), 5.36 (d, 1H, CH_2, $H_{f,Me,i}$), 4.72 (d, 1H, CH_2, $H_{f,Me,o}$), 4.56 (d, 1H, CH_2, $H_{f,NCMe,o}$), 4.52 (d, 1H, CH_2, $H_{c,Me,o}$), 4.50 (d, 1H, CH_2, $H_{c,NCMe,o}$), 3.64 (d, 1H, CH_2, $H_{c,Me,i}$), 3.30 (d, 1H, CH_2, $H_{c,NCMe,i}$), 2.18 (s, 3H, *Me*CN), 1.40 (s, 9H, *t*-Bu_c), 1.24 (s, 9H, *t*-Bu_f), 0.57 (s, 3H, Pd-Me). Selected ^{1}H−^{1}H NOESY correlations for **3a**: *δ* 1.31 with *δ* 4.54, 4.68, 7.02, and 7.08; for **3b**: *δ* 1.24 with *δ* 4.56, 4.72, 6.98, and 7.12, *δ* 1.40 with *δ* 0.57, 3.64, and 4.50. ^{13}C NMR (CD_2Cl_2, −60 °C):[16] **3a** *δ* 160.38, 159.80 ($C_{o\text{-}Py}$), 27.61 (C(*C*H_3)$_3$), 3.86 (*Me*CN), −5.39 (Pd-Me); **3b** *δ* 162.66, 162.40, 159.91, 158.54 ($C_{o\text{-}Py}$), 27.46 (C(*C*H_3)$_3$), 3.86 (*Me*CN), −8.05 (Pd-Me); **3a** + **3b** *δ* 139.29, 138.88, 138.85, 138.39 ($C_{p\text{-}Py}$), 124.84, 124.50, 124.37, 124.31, 122.99, 120.80 ($C_{m\text{-}Py}$), 63.35, 62.02, 60.82, 59.20, 58.00, 57.58, 57.29, 57.09, 56.79 (*C*H_2 and *C*(*C*H_3)$_3$). Anal. Calcd for $C_{57}H_{50}BF_{24}N_5Pd$: C, 49.67; H, 3.66; N, 5.08. Found: C, 49.53; H, 3.59; N, 4.78.

Compound (*t*-Bu-N_4)PdMe(C_2H_4)$^+$$BAr_4^-$ (4). This complex was generated in situ in CD_2Cl_2. A 15 mg sample of **3** was dissolved in 0.4 mL of CD_2Cl_2, and the solution was placed in an NMR tube and cooled to ca. −20 °C. Ethylene was then introduced at the top of the solution during a few seconds at ambient temperature, and the NMR tube was sealed, cooled to −80 °C, and vigorously shaken at this temperature. ^{1}H NMR analysis at −60 °C revealed that most of **3** had not yet reacted at this stage (low amounts of decomposition products were however detectable) and that 5 equiv of ethylene was present in solution. On raising the temperature, formation of complex **4** started above −40 °C and could be followed by ^{1}H NMR. Almost complete conversion was achieved after ca. 1 h at −30 °C, without further decomposition of **4**. The complex could then be analyzed by VT ^{1}H NMR between −90 and −20 °C. On raising the temperature above −10 °C, slow decomposition of **4** begun to occur, which was accelerated at higher temperature. ^{1}H NMR (CD_2Cl_2, −30 °C):[7,16] *δ* 7.48 and 7.41 (m, 1H, $H_{p\text{-}Py}$), 7.13 and 7.02 (d, 1H, $H_{m\text{-}Py,f}$), 6.97 and 6.86 (d, 1H, $H_{m\text{-}Py,c}$), 4.83 (d, 1H, CH_2, $H_{f,i}$), 4.76 (d, 1H, CH_2, $H_{c,o}$), 4.70 (d, 1H, CH_2, $H_{f,o}$), 4.59 (d, 1H, CH_2, $H_{c,o}$), 4.40 (d, 1H, CH_2, $H_{f,i}$), 4.38 (d, 1H, CH_2, $H_{f,o}$), 4.29 (m, 4H, C_2H_4), 3.68 and 3.51 (d, 1H, CH_2, $H_{c,i}$), 1.44 (s, 9H, *t*-Bu_c), 1.29 (s, 9H, *t*-Bu_f), 0.67 (s, 3H, Pd-Me). Selected ^{1}H−^{1}H COSY correlations: *δ* 1.29 with *δ* 4.70 and 4.38; *δ* 6.86 with *δ* 7.48, 7.13, 4.59, and 3.51; *δ* 6.97 with *δ* 7.41, 7.02, and 4.76. It could not be determined which protons of the macrocycle are located on the side of Me or C_2H_4 ligands.

X-ray Structures for 1 and 3. The X-ray structure determinations were carried out by the Service Commun de Rayons X de la Faculté de Chimie de Strasbourg. The structures were solved using direct methods and the Nonius MoleN Package for all calculations and refined by full-matrix least-squares. The experimental data are collected in Table 1.

Polymerization Experiments. The ethylene polymerization attempts were performed in a 1 L Buchi reactor equipped with a mechanical stirrer. The catalyst was first introduced into the reactor under argon as a toluene or a dichloromethane (for **3**) solution of controlled volume and concentration. The reactor was then filled with ethylene, and, in the case of **1**,

(16) The ^{1}H and ^{13}C NMR data for BAr_4^- are identical to those reported previously.[3f]

MAO was added under an ethylene flow with use of a syringe. The reactor was then pressurized with ethylene and the pressure maintained constant during the experiment. The addition of MAO to **1**/ethylene, and of ethylene to **3**, was followed by immediate fading of the solution and precipitation of metallic palladium. The reactions with hex-1-ene were performed using standard Schlenk techniques (0.05 mmol of **3**, 5 mL of toluene, 2.5 mL of hex-1-ene, 2 h). After quenching the reactions between **3** and ethylene or hex-1-ene by addition of a 10% solution of aqueous HCl in methanol, metallic palladium was separated by centrifugation and the solutions were analyzed by GC before they were evaporated to dryness (no significant residue was obtained in any case).

Acknowledgment. We are grateful to Mrs N. Kyritsakas and Dr. A. De Cian for the X-ray analyses, to R. Graf and J.-D. Sauer for running the 2D NMR experiments, and to the late Prof. J. A. Osborn for his support. We thank the CNRS for financial support (Program Catalyse et Catalyseurs pour l'Industrie et l'Environnement). S.P.M. is indebted to the Brazilian Government (CAPES) for a fellowship.

Supporting Information Available: Crystallographic data for **1**, **3**, and (Ts-N_4)$PdCl_2$; 2D NMR spectra for **3** and **4**. This material is available free of charge via the Internet at http://pubs.acs.org.

OM010475E